Progress In Electromagnetics Research, PIER 92, 347–360, 2009

SYNTHESIS OF PHASED ARRAYS IN COMPLEX ENVIRONMENTS WITH THE MULTILEVEL CHARACTERISTIC BASIS FUNCTION METHOD

J. Laviada, R. Ayestarán, M. R. Pino, and F. Las-Heras

Department of Electrical Engineering
Universidad de Oviedo
Campus Universitario, Gijón, Asturias 33203, Spain

R. Mittra

Department of Electrical Engineering
Penn State University
University Park, PA 16802-2705, USA

Abstract—The aim of this paper is to present a method to carry out the synthesis of large phased arrays when they are affected by complex environments which can influence the radiation pattern. The synthesis is performed with the help of the Multilevel Characteristic Basis Function Method to calculate a matrix relating input voltages and the far field pattern samples. The method is illustrated with the synthesis of a Secondary Surveillance Radar antenna on a turret containing multiple obstacles.

1. INTRODUCTION

Phased arrays for the problem of pattern synthesis is a challenging field, and multiple methods have been proposed in the past (e.g. [1–3]) where labels between brackets are references to the new papers included in the references section. The goal of the synthesis process is to realize a radiation pattern with certain characteristics that are typically defined by masks. The process has been traditionally carried out by using different types of approximations. The most common approximation has been to neglect the coupling between the elements

Corresponding author: J. Laviada (jlaviada@tsc.uniovi.es).

of the array and, therefore, to try to optimize the array factor (e.g., [4]).

Some authors have gone further and have incorporated full-wave methods to the synthesis process [5]. For instance, we can find some recent works with the incorporation of Neural Networks [6] or Support Vector Machines [7] to obtain a realistic model of the problem from measured data. However, these techniques depend on the conventional full-wave methods (e.g., Method of Moments, Finite Element Method, Finite Difference Time Domain, etc.) upon which they are based, or on the availability of large measured data sets.

Currently, acceleration schemes combined with the current computational resources are powerful enough to analyze large structures that were not amenable to rigorous analysis in the past. Thus, full-wave analyses of devices operating in complex environments have become possible by using techniques such as the Fast Multipole Method [8] or the Adaptive Integral Method [9]. Another interesting research line that has been recently exploited is the direct solution of the Method of Moments equations for electrically large problems, which will be especially important in the process that we consider. Among these acceleration techniques, we can cite the Multilevel MDA-CBI [10], the Mercury-MoM code [11] based on the Adaptive Cross Algorithm or the Characteristic Basis Function Method [12–15]. The latter plays a key role in the synthesis scheme proposed herein.

This paper presents a synthesis technique that employs a characterization of the antenna and its environment via an efficient application of a direct solution full-wave method. The remainder of this paper is arranged as follows: first, we perform the characterization of the radiation system; next, we detail the full-wave method as well as its modifications; finally, the synthesis procedure of a Secondary Surveillance Radar antenna is presented.

2. EFFICIENT CHARACTERIZATION OF THE PHASED ARRAY AND THE ENVIRONMENT

Most, if not all, of the aforementioned methods for the synthesis of phased arrays are based on the minimization of a cost function. This cost function typically requires the evaluation of the field radiated by a certain combination of voltages. For instance, the following cost function is minimized in [4]:

$$F(\mathbf{V}) = \|\mathbf{E}_{\text{target}} - \mathbf{E}(\mathbf{V})\|_2 + \alpha \|\mathbf{V}\|_2^2, \tag{1}$$

where $\mathbf{E}(\mathbf{V})$ is the aforementioned function that relates several field samples of a certain component (e.g., x-component of the field) with

the voltages applied to each element of the array, which are arranged in the vector $\mathbf{V}$. Parameter α controls the weight of each term. Thus, it is very convenient a quick evaluation of this kind of function.

Linearity of Maxwell's equations guarantees the existence of a unique matrix that relates the excitation vector with a certain component of the field. For instance, the θ-component of the field in a certain set of spatial points $\vec{r}_1, \vec{r}_2, \ldots, \vec{r}_M$ can be expressed as:

$$\begin{pmatrix} E_\theta(\vec{r}_1) \\ E_\theta(\vec{r}_2) \\ \vdots \\ E_\theta(\vec{r}_M) \end{pmatrix} = \begin{pmatrix} G_{11} & G_{12} & \ldots & G_{1N} \\ G_{21} & G_{22} & \ldots & G_{MN} \\ \vdots & \vdots & \ddots & \vdots \\ G_{M1} & G_{M2} & \ldots & G_{MN} \end{pmatrix} \begin{pmatrix} V_1 \\ V_2 \\ \vdots \\ V_N \end{pmatrix}. \quad (2)$$

Equation (2) can be expressed in a compact form by using the following the matrix equation:

$$\mathbf{E}_\theta = \mathbf{G}\mathbf{V}. \quad (3)$$

The matrix $\mathbf{G}$ can be calculated with the help of the superposition principle. Thus, the i-th column is computed by exciting with an unitary source the i-th source and setting the rest at zero. The obtained field samples of the θ-component at the sample points will form the i-th column of the matrix.

Since the previous process is repeated for each element of the array, we need to handle multiple right hand sides. For this reason, if the array contains many elements and the environment is larger, acceleration schemes based on iterative process (e.g., GMRES or conjugated gradient) are not well suited for this task, because they must repeat the entire process for each right hand side.

3. APPLICATION OF THE ML-CBFM TO THE SYNTHESIS PROCESS

The Method of Moments (MoM) expands an unknown current on a series of basis functions $\vec{f}_n$:

$$\vec{J} = \sum_n I_n \vec{f}_n. \quad (4)$$

The insertion of the previous equation into an integral equation yields a matrix equation of the form:

$$\mathbf{Z}\mathbf{I} = \mathbf{V}. \quad (5)$$

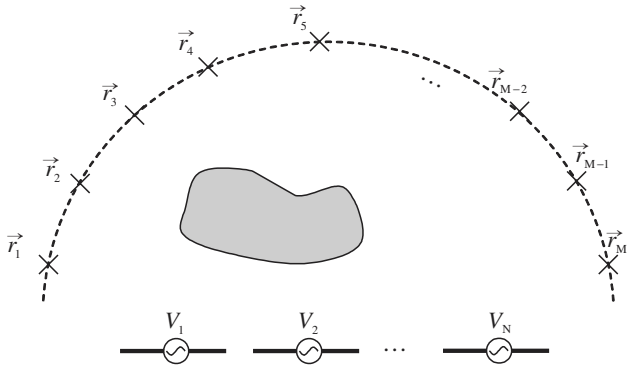

Figure 1. Phased array in an environment and some field samples points.

One important thing to notice is that the excitation only affects the right hand side of the equation. If the matrix is small enough, Eq. (4) can be efficiently solved by factorizing the matrix. Once the factorization has been performed, if only the right hand side is changed, then (5) can be solved taking advantage of this factorization. Hence, multiple right hand sides can be solved again efficiently if the matrix can be factorized. This is known as the direct solution.

However, the factorization typically requires us to store the full dense matrix into the available memory so it requires a memory complexity $\mathcal{O}\left(N^2\right)$. In addition, it becomes very time consuming for relatively large problems owing to the time complexity $\mathcal{O}\left(N^3\right)$. Thus, the size of the problem that can be solved by this method is very limited. The Characteristic Basis Functions Method (CBFM) defines a new set of basis functions, which enables us to represent the current using a smaller number of unknowns. This is possible by exploiting the underlying physics. Hence, this method enables us to directly solve a relatively large set of problems, because the size of the reduced matrix is small. This strategy has been further extended to achieve higher compression rates by applying the CBFM over the existing CBFs, which now play the role of the conventional low-level basis functions. This methodology is known as the ML-CBFM [16] and is used in this paper.

We describe here how a two level ML-CBFM must be modified to be applied to the synthesis of phased arrays. The ML-CBFM splits the geometry into several blocks (groups of adjacent basis functions) where several high-level CBFs are defined. Thus, the current is expressed as a linear combination of the CBFs of these large-size subdomains (blocks),

by expressing (4) as:

$$\vec{J} = \sum_{b=1}^{B} \sum_{n=1}^{N_b} I_{b,n} \vec{\mathcal{F}}_{b,n}, \tag{6}$$

where B is the number of second-level blocks; N_b is the number of CBFs in the b-th block; and the coefficients I are the unknowns to be calculated with the MoM. Each second-level CBF is defined in terms of the first-level CBFs as:

$$\vec{\mathcal{F}}_{b,n} = \sum_{c=1}^{B_b} \sum_{m=1}^{N_{\{b,c\}}} I^{(n)}_{\{b,c\},m} \vec{\mathcal{F}}_{\{b,c\},m}, \tag{7}$$

being B_b the number of first-level blocks inside the b-th second-level block; $N_{b,c}$ are the number of first-level CBFs; $I^{(n)}_{\{b,c\},m}$ are the weights of the first-level CBFs; and $\vec{\mathcal{F}}_{\{b,c\},m}$ are the first-level CBFs. Finally, first-level CBFs are defined in terms of low-level basis functions as usual:

$$\vec{\mathcal{F}}_{\{b,c\},m} = \sum_{l=1}^{N^{(0)}_{\{b,c\}}} I^{(m)}_{\{b,c,l\}} \vec{f}_{\{b,c\},l}, \tag{8}$$

where $N^{(0)}_{\{b,c\}}$ are the number of low-level basis functions in the block $\{b,c\}$; $I^{(n)}_{\{b,c,l\}}$ are the weights of the low-level basis functions; and $\vec{f}_{\{b,c\},l}$ are the low-level basis functions in the block $\{b,c\}$.

The calculation of the coefficients $I^{(n)}_{\{b,c,l\}}$ and $I^{(n)}_{\{b,c\},m}$, which define the first-level and second-level CBFs, respectively, is carried out by progressing from lowest to the highest level stepping out one level at a time. Several approaches have been employed in the past to define the CBFs, and we will use the one detailed in [14] not only because it is well-suited for large structures but because it also yields CBFs that are independent of the other blocks. This approach was originally defined for scattering problems and we modify it slightly to analyze the antennas. Next, we define how it can be easily extended to the synthesis problem at hand.

To generate the CBFs, we consider the electric field integral equation (EFIE) for a perfect electric conductor:

$$\vec{E}_i + \vec{E}_s\Big|_t = 0, \tag{9}$$

where $\vec{E}_i$ the impressed and $\vec{E}_s$ is the scattered field, respectively. The latter can be expressed in terms of the induced currents, $\vec{J}$, using a linear operator $\mathcal{L}(\cdot)$ notation as:

$$\vec{E}_s = \mathcal{L}\left(\vec{J}\right). \tag{10}$$

Let us assume that the induced currents in all the blocks except the n-th are known. Hence, Eq. (9) becomes:

$$-\mathcal{L}\left(\vec{J}_n\right)\Big|_t = \vec{E}_i + \sum_{\substack{m=1 \\ m\neq n}}^{B} \mathcal{L}\left(\vec{J}_m\right)\Bigg|_t. \tag{11}$$

Solving the previous integral equation would give us the final current on this block. It is important to realize that by invoking the superposition principle, we can regard the final current on a block as a *linear combination* of the currents induced by the radiation of the blocks plus the current induced by the impressed field.

Previous approaches as [14, 15], which were focused on scattering problems, employed plane waves in the visible spectrum to approximate the field external to the block. Since the impressed fields were plane waves for the computation of RCS, then modeling of the external field due to the external geometry and the impressed field could be performed at the same time without further processing.

It is also important to remark that the number of plane waves is typically determined, and the coefficients of the currents induced in the block are filtered with a singular value decomposition (SVD). Since some blocks can also have an impressed field internal to them, we must also consider the currents induced by a source internal to the block, such as a delta-gap or a magnetic thrill.

Thus, if we consider the c-th first-level block inside the b-th second-level block (denoted by $\{b,c\}$), which contains S_i internal sources, in order to calculate the CBFs, we build the following matrix:

$$\mathbf{W} = \begin{bmatrix} P^{(1)}_{\{b,c\},1} & \cdots & P^{(N_{PW})}_{\{b,c\},1} & Q^{(1)}_{\{b,c\},1} & \cdots & Q^{(S_{\{b,c\}})}_{\{b,c\},1} \\ \vdots & \ddots & \vdots & \vdots & \ddots & \vdots \\ P^{(1)}_{\{b,c\},N_{\{b,c\}}} & \cdots & P^{(N_{PW})}_{\{b,c\},N_{\{b,c\}}} & Q^{(1)}_{\{b,c\},N_{\{b,c\}}} & \cdots & Q^{(S_{\{b,c\}})}_{\{b,c\},N_{\{b,c\}}} \end{bmatrix} \tag{12}$$

where the coefficients P are the weights of the low-level basis functions when the block is excited with a plane wave and the coefficients Q are the same weights but in the case of using an internal source. This

matrix is factorized as in [14] with an SVD in order to retain the most significant combinations, which will be used as the final first-level CBFs.

After computing the first-level CBFs, the calculation of the second-level CBFs is analogous. In this case, the matrix to be factorized of the b-th second-level block is built as:

$$\mathbf{W} = [\ \mathbf{P} \quad \mathbf{Q}\ ] \tag{13}$$

where the previous matrices are defined as:

$$\mathbf{P} = \begin{bmatrix} P^{(1)}_{\{b,1\},1} & \cdots & P^{(N_{PW})}_{\{b,1\},1} \\ \vdots & \ddots & \vdots \\ P^{(1)}_{\{b,1\},N_{\{b,1\}}} & \cdots & P^{(N_{PW})}_{\{b,1\},N_{\{b,1\}}} \\ P^{(1)}_{\{b,2\},1} & \cdots & P^{(N_{PW})}_{\{b,2\},1} \\ \vdots & \ddots & \vdots \\ P^{(1)}_{\{b,B_b\},N_{\{b,B_b\}}} & \cdots & P^{(N_{PW})}_{\{b,B_b\},N_{\{b,B_b\}}} \end{bmatrix} \tag{14}$$

$$\mathbf{Q} = \begin{bmatrix} Q^{(1)}_{\{b,1\},1} & \cdots & Q^{(S_b)}_{\{b,1\},1} \\ \vdots & \ddots & \vdots \\ Q^{(1)}_{\{b,1\},N_{\{b,1\}}} & \cdots & Q^{(S_b)}_{\{b,1\},N_{\{b,1\}}} \\ Q^{(1)}_{\{b,2\},1} & \cdots & Q^{(S_b)}_{\{b,2\},1} \\ \vdots & \ddots & \vdots \\ Q^{(1)}_{\{b,B_b\},N_{\{b,B_b\}}} & \cdots & Q^{(S_b)}_{\{b,B_b\},N_{\{b,B_b\}}} \end{bmatrix} \tag{15}$$

where S_b are the internal sources in the second-level block; the coefficients P are the weights of the first-level basis functions when the block is excited with a plane wave and the coefficients Q are the same weights but in the case of using an internal source.

Currents induced by several plane waves as well as by a delta-gap on a monopole mounted on a circular platform are shown in Fig. 2. It shows that, in general, the currents induced by plane waves display a different behaviour when it compared to the current induced by an internal voltage source. Hence, it is important to take into account this type of current in the process of generating the CBFs.

Once the CBFs have been calculated, (6) is introduced in the EFIE to calculate the system matrix which is solved to obtain the coefficients of the final currents.

4. NUMERICAL RESULTS

To illustrate the aforementioned process, we consider a Secondary Surveillance Radar (SSR) Antenna. This kind of antennas requires a narrow main lobe in azimuth to make sure that the antenna is not interrogating more than one target at the same time. Elevation diagram corresponds to a square cosine in the area of interest to ensure the same echo amplitude while the target is approaching the antenna. This kind of antenna is typically situated on high positions for a better visibility. Among the elements that can be found in the proximities of a SSR antenna, we can cite primary radar antennas, anemometers or lighting rods.

We model an antenna based on the commercial antenna CSL-20L of CESELSA company with 10 rows and 33 columns of half-wavelength dipoles. The length of the model is 8 m and the height is 1 m. We employ the excitations calculated in [17] as the nominal excitations. This excitation is modeled as a separable distribution for each direction. The nominal voltages are shown in Fig. 3 (vertical distribution has a zero phase and it is omitted).

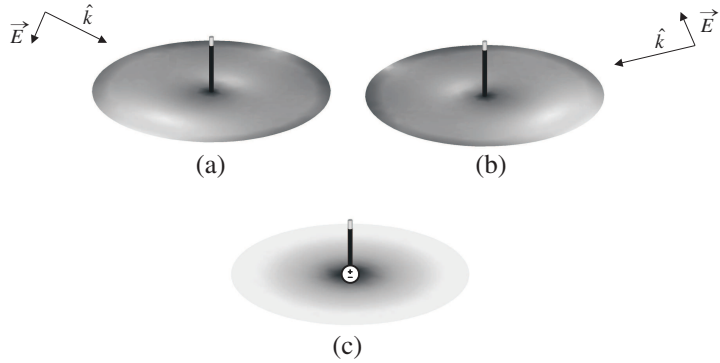

Figure 2. Currents induced by different plane waves and a delta-gap source for a monopole mounted on a circular platform.

The geometry model with the fastening system is shown in Fig. 4. Radiation patterns for the azimuth and elevation are shown in Fig. 5. It is observed that the radiation pattern fulfills the mask requirements.

Next, we include the environment of the antenna as shown in Fig. 6. This environment includes the supporting ground, a primary radar and several lighting rod poles. Since the most critical and strict radiation pattern is the one for the azimuth sweep, we will focus in this plane for the synthesis process. The radiation pattern modified after

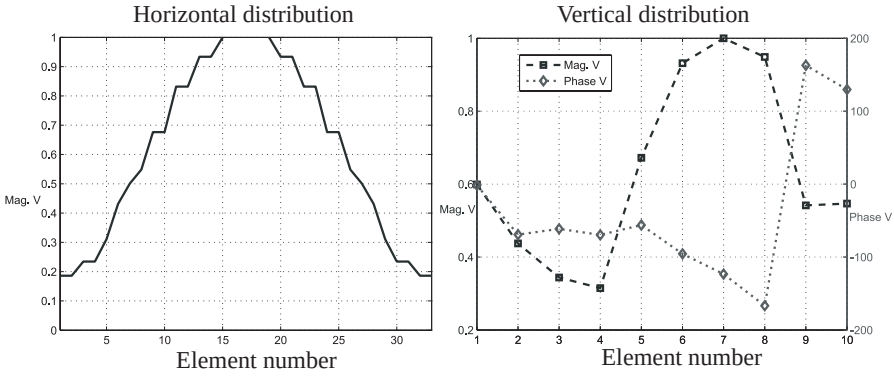

Figure 3. Nominal excitations of the array: horizontal distribution (left), vertical distribution (right).

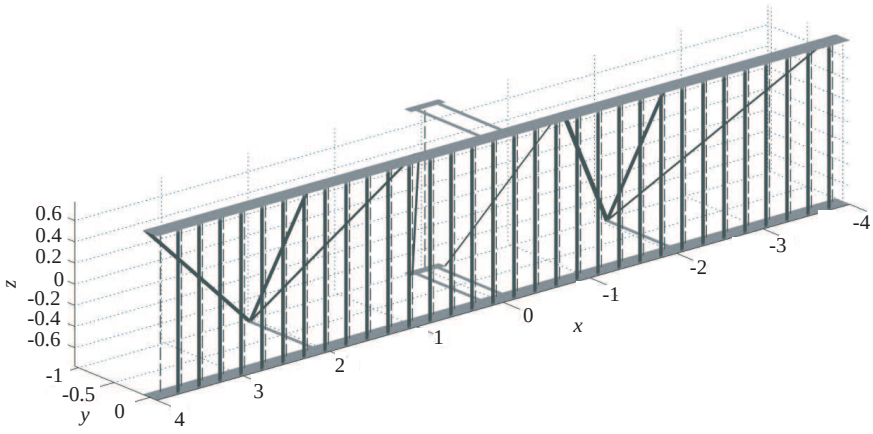

Figure 4. Phased array and the fastening system.

taking into account the environment is shown in Fig. 7.

In order to apply the ML-CBFM, the geometry of Fig. 7 is decomposed into six blocks: one for the entire SSR antenna, one for the primary radar reflector and the four remaining blocks are used to model the rest of the geometry in a symmetric way. The generation of the CBFs is carried out by illuminating the blocks with 6,720 plane waves and filtering the currents with an SVD threshold set at 10^{-3} for the first-level and 10^{-4} for the second-level.

The geometry is discretized with the help of 139,762 RWG basis functions that are compressed to 20,259 after the first application of

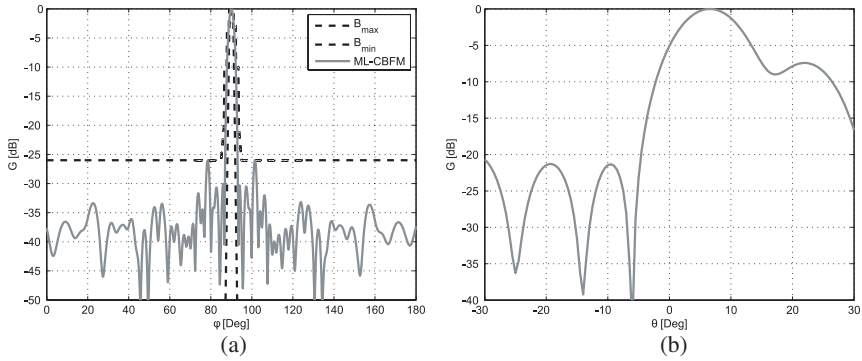

Figure 5. Azimuth (left) and elevation (right) radiation patterns for the SSR antenna with the fastening system.

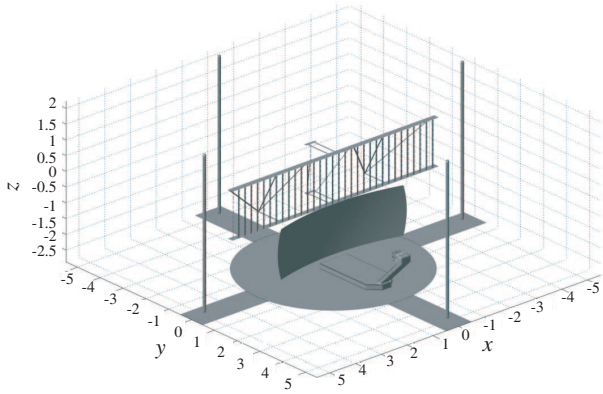

Figure 6. SSR antenna with the environment composed by the supporting ground, a primary radar and four lighting rods.

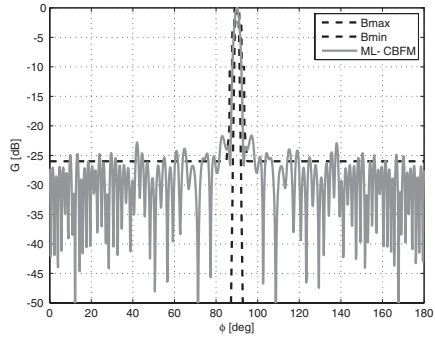

Figure 7. Azimuth radiation pattern of the SSR antenna with the environment for the nominal excitations.

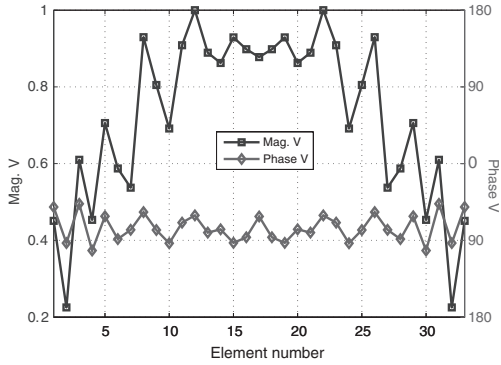

Figure 8. Synthesized excitations for the SSR antenna with the environment.

the CBFM, and to 13,312 after the second.

For the synthesis process, we employ the iterative process described in [7] with the exception that the G matrix has been calculated with the aforementioned method instead of using Support Vectors Machines. The method converges to a radiation pattern with two peaks of 1.5 dB over the mask after only a few iterations. For this reason, we make a further optimization by employing a simulated annealing where the cost function is defined as the area of the radiation pattern which is outside the masks. The synthezised excitations are shown in Fig. 8.

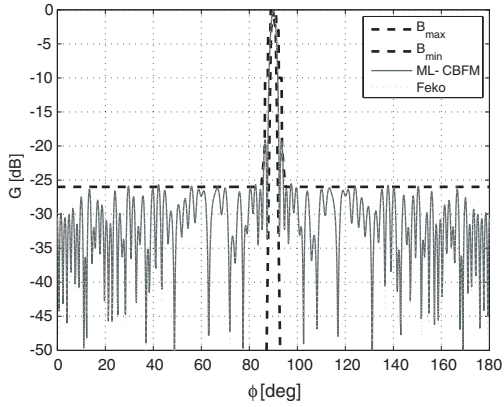

Figure 9. Azimuth radiation pattern of the SSR antenna with the environment after the synthesis process.

The achieved radiation pattern has a maximum difference of 0.37 dB over the mask and is shown in Fig. 9. The results have been validated with the commercial software Feko [18], which utilizes the MLFMA algorithm (iterative). The agreement between the two results is seen to be very good.

5. CONCLUSIONS

A method for the efficient calculation of a matrix for the correct modeling of a phased array in terms of voltages and field samples has been presented. The simulation of the array has been carried out by using the full-wave method called ML-CBFM, which has been adapted to the problem at hand. Once this matrix has been generated, it can be used for a wide variety of synthesis problems. To illustrate our scheme, the optimization of a SSR antenna radiation pattern, which is a phased array, has been performed for the case where the radiation pattern of the array has seen a modification because of its environment.

ACKNOWLEDGMENT

This work has been supported by Ministerio de Ciencia e Innovacin of Spain/FEDER under projects TEC2008-01638/TEC (INVEMTA) and CONSOLIDER-INGENIO CSD2008-00068 (TERASENSE); by Unin Europea-Fondo Europeo de Desarrollo Regional under project EQP06-015; by Gobierno del Principado de Asturias-Plan de Ciencia y Tecnologa (PCTI)/FEDER-FSE under grant BP06-101 and by Ctedra Telefnica-Universidad de Oviedo.

REFERENCES

1. Liu, Z. F., P. S. Kooi, L. W. Li, M. S. Leong, and T. S. Yeo, "A method of moments analysis of a microstrip phased array in three layered structures," *Progress In Electromagnetic Research*, PIER 31, 155–179, 2001.
2. Yuan, T., L.-W. Li, and M.-S. Leong, "Efficient analysis and design of finite phased arrays of printed dipoles using fast algorithm: Some case studies," *Journal of Electromagnetic Waves and Applications*, Vol. 21, No. 6, 737–754, 2007.
3. Hassani, H. R. and M. Jahanbakht, "Method of moment analysis of finite phased array of aperture coupled circular microstrip patch antennas," *Progress In Electromagnetics Research B*, Vol. 4, 197–210, 2008.

4. Ares, F. M., J. A. Rodríguez, E. Villanueva, and S. R. Rengajaran, "Genetic algorithms in the design and optimization of antenna array pattern," *IEEE Trans. Antennas Propagat.*, Vol. 47, 506–510, 1999.
5. Landesa, L., F. Obelleiro, J. L. Rodriguez, and A. G. Pino, "Pattern synthesis of array antennas in presence of conducting bodies of arbitrary shape," *Electronics Letters*, Vol. 33, 1512–1513, 1997.
6. Ayestaran, R. G., F. Las-Heras, and L. F. Herran, "Neural modeling of mutual coupling for antenna array synthesis," *IEEE Trans. Antennas Propagat.*, Vol. 55, 832–840, 2007.
7. Ayestaran, R. G., M. F. Campillo, and F. Las-Heras, "Multiple support vector regression for antenna array characterization and synthesis," *IEEE Trans. Antennas Propagat.*, Vol. 55, No. 9, 2495–2501, 2007.
8. Coifman, R., V. Rokhlin, and S. Wandzura, "The fast multipole method for the wave equation: A pedestrian prescription," *IEEE Trans. Antennas Propagat. Mag.*, Vol. 53, 7–12, 1993.
9. Bleszynski, E., M. Bleszynski, and T. Jaroszewicz, "AIM: Adaptive integral method for solving large-scale electromagnetic scattering and radiation problems," *Radio Sci.*, Vol. 31, 1225–1251, 1996.
10. Heldring, A., J. M. Rius, J.-M. Tamayo, J. Parron, and E. Ubeda, "Fast direct solution of method of moments linear system," *IEEE Trans. Antennas Propagat.*, Vol. 55, No. 11, 3220–3228, 2007.
11. Shaeffer, J., "Direct solve of electrically large integral equations for problem sizes to 1 M unknowns," *IEEE Trans. Antennas Propagat.*, Vol. 56, No. 8, 2306–2313, 2008.
12. Prakash, V. and R. Mittra, "Characteristic basis function method: A new technique for efficient solution of method of moments matrix equation," *Microwave Opt. Technol. Lett.*, Vol. 36, 95–100, 2003.
13. Mittra, R. and K. Du, "Characteristic basis function method for iteration-free solution of large method of moments problems," *Progress In Electromagnetics Research B*, Vol. 6, 307–336, 2008.
14. Lucente, E., A. Monorchio, and R. Mittra, "An iteration-free MoM approach based on excitation independent characteristic basis functions for solving large multiscale electromagnetic scattering problems," *IEEE Trans. Antennas Propagat.*, Vol. 56, 999–1007, 2008.
15. Delgado, C., M. F. Cátedra, and R. Mittra, "Application of

the characteristic basis function method utilizing a class of basis and testing functions defined on NURBS patches," *IEEE Trans. Antennas Propagat.*, Vol. 56, 784–791, 2008.

16. Laviada, J., F. Las-Heras, M. R. Pino, and R. Mittra, "Generation of nested characteristic basis functions," *Proc. of European Conference on Antennas and Propagation (EuCAP 2009)*, Berlin, Germany, Mar. 23–27, 2009.
17. Las-Heras, F., B. Galocha, and J. L. Besada, "Equivalent source modelling and reconstruction for antenna measurement and synthesis," *Proc. IEEE AP-S International Symposium, Montreal*, Vol. 1, 156–159, Canada, July 13–18, 1997.
18. Van Tonder, J. and U. Jakobus, "Fast multipole solution of metallic and dielectric scattering problems in Feko," *Proc. 21st Annual Review of Progress in Applied Computational Electromagnetics*, ACES, Hawaii, 2005.